Published in final edited form as:
*Cell Host Microbe*. 2012 December 13; 12(6): 778–790. doi:10.1016/j.chom.2012.10.019.

# The LRR and RING Domain Protein LRSAM1 Is an E3 Ligase Crucial for Ubiquitin-Dependent Autophagy of Intracellular *Salmonella* Typhimurium

**Alan Huett**[1,2,6,8], **Robert J. Heath**[1,2,3,6], **Jakob Begun**[1,2,7], **Slim O. Sassi**[1,4,7], **Leigh A. Baxt**[5], **Jatin M. Vyas**[5], **Marcia B. Goldberg**[5], and **Ramnik J. Xavier**[1,2,3,*]

[1]Center for Computational and Integrative Biology

[2]Gastrointestinal Unit and Center for the Study of Inflammatory Bowel Disease Massachusetts General Hospital, Boston, MA 02114, USA

[3]The Broad Institute of MIT and Harvard, Cambridge, MA 02142, USA

[4]Department of Genetics, Harvard Medical School, Boston, MA 02115, USA

[5]Department of Medicine, Division of Infectious Diseases, Massachusetts General Hospital, Cambridge, MA 02139, USA

## SUMMARY

Several species of pathogenic bacteria replicate within an intracellular vacuolar niche. Bacteria that escape into the cytosol are captured by the autophagic pathway and targeted for lysosomal degradation, representing a defense against bacterial exploitation of the host cytosol. Autophagic capture of *Salmonella* Typhimurium occurs predominantly via generation of a polyubiquitin signal around cytosolic bacteria, binding of adaptor proteins, and recruitment of autophagic machinery. However, the components mediating bacterial target selection and ubiquitination remain obscure. We identify LRSAM1 as the E3 ligase responsible for anti-*Salmonella* autophagy-associated ubiquitination. LRSAM1 localizes to several intracellular bacterial pathogens and generates the bacteria-associated ubiquitin signal; these functions require LRSAM1's leucine-rich repeat and RING domains, respectively. Using cells from LRSAM1-deficient individuals, we confirm that LRSAM1 is required for ubiquitination associated with intracellular bacteria but dispensable for ubiquitination of aggregated proteins. LRSAM1 is therefore a bacterial recognition protein and ubiquitin ligase that defends the cytoplasm from invasive pathogens.

## INTRODUCTION

A number of pathogenic bacteria adopt an intracellular lifestyle to escape extracellular immune responses and replicate within a protected niche. One such species is *Salmonella* Typhimurium, which is capable of invading epithelial cells and replicating within a host-derived membrane vacuole. Bacteria that escape from these *Salmonella*-containing vacuoles



*Correspondence: xavier@molbio.mgh.harvard.edu.
[6]These authors contributed equally to this work
[7]These authors contributed equally to this work
[8]Present address: School of Biology, University of Nottingham, University Park, Nottingham, NG7 2RD, UK

**SUPPLEMENTAL INFORMATION**

Supplemental Information includes seven figures, Supplemental Experimental Procedures, and one movie and can be found with this article online at http://dx.doi.org/10.1016/j.chom.2012.10.019.

(SCVs) into the cytosol are captured by the autophagic pathway. Autophagy therefore represents a barrier to bacterial exploitation of the host cytosol, enabling the cell to sequester deleterious cargos within a double-membrane compartment termed the autophagosome. Following cargo capture, autophagosomes fuse with lysosomes to degrade their contents.

Autophagic capture of bacteria occurs via at least two known routes. The first is a ubiquitin-dependent process in which bacteria are surrounded by a coat of polyubiquitin. The ubiquitinated coat is bound by ubiquitin interacting autophagy adaptor proteins (e.g., NDP52 and p62), resulting in recruitment of autophagic machinery (Shaid et al., 2012). The second route is ubiquitin independent and relies on production of diacylglycerol (DAG) in membranes surrounding the bacteria (Shahnazari et al., 2010). The signals and adaptor proteins involved in this pathway are yet to be fully defined. In the case of *S.* Typhimurium, the ubiquitin-dependent pathway dominates under most conditions (Shahnazari et al., 2010). Recently, a role for galectin-8 in sensing vacuolar damage induced by *S.* Typhimurium was discovered (Thurston et al., 2012). The authors propose a model whereby the autophagy adaptor protein NDP52 is recruited by galectin-8 in a transient fashion to damaged vacuoles, but persistence of NDP52 localization requires ubiquitination (Thurston et al., 2012). These data indicate that ubiquitination plays a key role in marking cytosol-exposed bacteria for autophagy.

Despite the importance of ubiquitination in degradation of bacteria, the components that mediate this process have not yet been characterized. Ubiquitination requires a tripartite complex of E1, E2, and E3 enzymes. E3s represent the most numerous and diverse group and are responsible for target selection. The majority of known E3 ligases are of the RING type, with some 600 representatives in the human genome (Deshaies and Joazeiro, 2009), but the targets of many remain undefined. We previously showed that the LRR-containing RING E3 ligase LRSAM1 was required for autophagy of *S.* Typhimurium in epithelial cells (Ng et al., 2011). The presence of an LRR domain (often a feature of innate pattern recognition receptors), and E3 ligase activity led us to postulate that LRSAM1 might be the E3 ligase involved in ubiquitin-dependent anti-*Salmonella* autophagy. Given the known role for LRSAM1 in endocytic and exocytic cargo sorting, we hypothesized an extension of this function to encompass autophagic cargo selection (Amit et al., 2004). In this study we further characterize the role and mechanism of LRSAM1 action and show that LRSAM1 is the E3 ligase responsible for bacteria-associated ubiquitination prior to autophagy and therefore drives the major antibacterial autophagy pathway. LRSAM1 recognizes bacteria via its LRR domain and promotes ubiquitination in a RING domaindependent manner without the need for other recognition or accessory proteins. We therefore propose that LRSAM1 is a pattern-recognizing E3 ligase in the autophagy pathway and is active against a range of intracellular bacteria.

## RESULTS

### LRSAM1 Localizes to Bacteria and Restricts Cytoplasmic Replication

We had previously observed that cells deficient for LRSAM1 were unable to mediate anti-*Salmonella* autophagy (Ng et al., 2011). However, the functions of LRSAM1 in this process remained unclear. To gain insight into the role of LRSAM1 in anti-*Salmonella* autophagy, we stained for endogenous LRSAM1 and the autophagosome marker LC3 during infection of HeLa cells with *S.* Typhimurium (Figure 1A). We observed a proportion of *S.* Typhimurium (5% ± 1.8%, means ± SEM from three independent experiments) colocalized with both LRSAM1 and LC3 at 45 min postinfection. We also stained for endogenous LRSAM1 during infection of HeLa cells with *S.* Typhimurium and other intracellular pathogenic bacteria (Figures 1B and 1C) and found that LRSAM1 extensively colocalized with bacteria. In HeLa cells, the rate of endogenous LRSAM1 localization to internalized *S.*

Typhimurium SL1344 was 10% ± 1.6% at 40 min following infection (mean ± SEM from three independent experiments). In addition, we observed LRSAM1 localization to internalized adherent invasive *Escherichia coli* (AIEC, 18% ± 3.9%), *Shigella flexneri* ΔIcsB (29% ± 5.3%), and *Listeria monocytogenes* EGDe (25% ± 6.2%)–all bacterial strains that are susceptible to autophagy (Figure 1B) (Lapaquette et al., 2010; Meyer-Morse et al., 2010; Ogawa et al., 2005). Colocalization was rarely seen between LRSAM1 and the autophagy-evading wild-type *S. flexneri* or *L. monocytogenes* 15313 (3% ± 1.5% and 4% ± 1.9% of internalized bacteria, respectively). LRSAM1 localization to *S.* Typhimurium was also seen in infected macrophages (Figure S1A). This broad correlation of LRSAM1 localization with antibacterial autophagy strongly suggested that LRSAM1 was important in the autophagy process, but it remained unclear whether LRSAM1 bacterial association was required for control of bacterial infection. We therefore confirmed that knockdown of LRSAM1 resulted in increased numbers of intracellular *Salmonella* (Figures 1D, S1B, and S1C), consistent with previous observations that loss of autophagy during *Salmonella* infection results in increased bacterial replication within epithelial cells (Huett et al., 2009; Kuballa et al., 2008; Lapaquette et al., 2010; Thurston et al., 2009). In the absence of LRSAM1, bacterial replication was increased to the same extent as with knockdown of ATG16L1 (Figure S1D), a protein crucial for antibacterial autophagy (Figure 1D) (Rioux et al., 2007), underlining the importance of LRSAM1 to autophagic degradation of this pathogen.

Upon infection of epithelial cells, *S.* Typhimurium resides in SCVs, which recruit lysosomal membrane proteins including LAMP1. The environment of the SCV serves as a protective niche, promoting bacterial survival and replication; bacteria that are released from SCVs and exposed to the cytosol become targets for ubiquitin association and degradation (Birmingham et al., 2006). LRSAM1 knockdown did not affect the efficiency of *S.* Typhimurium invasion into HeLa cells (Figure 1D, 1 hr time point), nor the proportion of bacteria initially within SCVs, as evidenced by equivalent LAMP1 staining of bacteria at 1 hr postinfection (Figures 1E and S1E). However, at 6 hr postinfection a significantly increased proportion of *Salmonella* in LRSAM1-depleted cells was LAMP1-negative, suggestive of exit from the SCV into the cytoplasm without subsequent destruction by autophagy (Figure 1E). We next directly quantified cytoplasmic *S.* Typhimurium using differential digitonin permeabilization and antibody staining of cytoplasmic bacteria (Malik-Kale et al., 2012) (Figures 1F and S1F). LRSAM1- and ATG16L1-knockdown cells had higher numbers of bacteria per cell than control cells at 6 hr postinfection, indicative of enhanced replication in the cytoplasm. When these data were examined in terms of the proportion of cytoplasmic bacteria compared to control cells, we further confirmed that both ATG16L1- and LRSAM1-deficient cells showed increased proportions of cytoplasmic bacteria with 56% ± 15% and 57% ± 16% of total internalized bacteria, respectively, compared to just 13% ± 3% in controls (means ± SEM from three independent experiments). Examples of LAMP1 and cytoplasmic anti-*Salmonella* staining are shown in Figures S1E and S1F. Investigation of the maturation status of SCVs revealed that LRSAM1 colocalizes with markers of the early maturation phase of the vacuolar compartment including Rab4, but not Rab11 or sorting nexin-3 (Figure 1G) (Birmingham et al., 2006; Braun et al., 2010; Smith et al., 2005). These data underlined a prominent role for LRSAM1 in antibacterial autophagy; we therefore set out to further investigate the role of LRSAM1 domains in the recognition and autophagy of bacteria.

## LRSAM1 Localizes to Bacteria via Its LRR Domain

To elucidate the mechanism of LRSAM1 action, we used an RNAi knockdown/rescue strategy. We generated a series of siRNA-resistant constructs to express full-length or truncated LRSAM1 during knockdown of endogenous protein (Figure 2A). Cotransfection of these constructs with control siRNA duplexes demonstrated no significant effect of

LRSAM1 construct expression on anti-*Salmonella* autophagy (Figure 2B). LRSAM1 knockdown resulted in loss of anti-*Salmonella* autophagy, which was rescued by expression of the full-length LRSAM1 protein, but not by ΔLRR or ΔRING domain mutants (Figures 2C and 2D). Examination of the localization of these mutants during *S.* Typhimurium infection showed that in cells expressing solely LRSAM1 ΔRING, LRSAM1 still localized to internalized bacteria (Figure 2E). In contrast, LRSAM1 ΔLRR did not associate with bacteria, despite equivalent cytoplasmic expression. This was also the case for the Δ190 mutant. In a reciprocal experiment, we observed that a truncated protein composed of only the N-terminal 190 amino acids (aa) of LRSAM1 (N190) efficiently localized to internalized bacteria (Figure 2E).

Given that the LRR was necessary and sufficient to mediate LRSAM1 localization, we hypothesized that the RING domain would be required to mediate ubiquitin association, and that loss of autophagy following LRSAM1 knockdown was due to a reduction in the association of ubiquitin with *Salmonella*. Staining of endogenous ubiquitin in HeLa cells expressing wild-type LRSAM1 showed that full-length LRSAM1 colocalized with ubiquitin around intracellular *Salmonella* (Figure 3A). Cells expressing solely LRSAM1 ΔRING did not show such ubiquitination, despite LRSAM1 ΔRING/*Salmonella* colocalization (Figure 3B). Expression of either ΔLRR or ΔRING constructs failed to restore bacterial ubiquitin association following LRSAM1 knockdown (Figure 3C), demonstrating that both LRR and RING domains are required for the colocalization of ubiquitin with bacteria in vivo.

It has been proposed that transient galectin-mediated NDP52 recruitment to *S.* Typhimurium occurs simultaneously with the recruitment of ubiquitin and autophagy adaptors around bacterial targets, with ubiquitin-dependent NDP52 recruitment dominating postinvasion events (Thurston et al., 2012). The kinetics of LRSAM1 recruitment on *S.* Typhimurium infection were consistent with this model; peak LRSAM1 localization to bacteria (40 min) occurred prior to peak bacterial ubiquitin and NDP52 colocalization (60 min) (Figure 3D). LRSAM1 has also been reported to bind to GABARAPL2, an ATG8-like molecule (Stelzl et al., 2005), suggesting that it might serve to recruit autophagosomal components directly. We therefore tested a number of autophagy proteins and ubiquitin-binding adaptors for LRSAM1 binding. Using coimmunoprecipitation, we observed an interaction between LRSAM1 and NDP52, but not GABARAPL2, LC3, or p62 (Figure 4A). These findings were confirmed using purified LRSAM1 protein to coprecipitate NDP52 from cell lysates (Figures 4B and 4C), and mixing of purified LRSAM1 and NDP52 proteins resulted in coelution from streptavidin beads (Figures 4D and 4E). Using truncations (Figure 4B), we found that the NDP52 SKICH domain (responsible for Nap1 interaction [Thurston et al., 2009]) and the ubiquitin-binding zinc finger domain are both dispensable for the LRSAM1/ NDP52 interaction. NDP52 aa 127–255 were essential for LRSAM1 binding (Figure 4F). Reciprocal analysis of LRSAM1 identified the LRR (aa 1–190) region as being required for NDP52 binding (Figures 4G and 4H). These results led us to conclude that there is an LRSAM1 LRR-binding surface in the aa 127–255 region of NDP52, separate from characterized binding sites for ubiquitin, Nap1, or galectin (Thurston et al., 2009, 2012), and that the LRSAM1/ NDP52 interaction is not dependent on mutual ubiquitin binding.

## LRSAM1 Localizes to Bacteria Independently of NDP52

Given the role for galectin-8 and NDP52 in the marking of bacteria that are targeted by autophagy, as well as our observed LRR-mediated binding of LRSAM1 to NDP52, we investigated whether LRSAM1 targeting to bacteria required NDP52. Staining of *S.* Typhimurium-infected cells for LRSAM1 and NDP52 showed both endogenous proteins localized to intracellular bacteria (Figures 5A, S2A, and S2B, Movie S1). However, although NDP52 and LRSAM1 each colocalized with bacteria, they appeared to localize to spatially separate subdomains around bacteria. We therefore directly tested the requirement

for NDP52 in LRSAM1 localization to bacteria by NDP52 knockdown (Figures S2C and S2D). NDP52 ablation did not hinder the localization of endogenous LRSAM1 to intracellular *Salmonella* at 40 min postinfection (siControl = 12.5% ± 1.9%; siNDP52 = 10.5% ± 1.8%; means ± SEM from three independent experiments), demonstrating that LRSAM1 localization is NDP52 independent (Figure 5B).

Together with data indicating that persistence of NDP52 localization to bacteria requires ubiquitination (Thurston et al., 2012), our findings suggest that functional LRSAM1 might also be required for persistent NDP52 and p62 recruitment to bacteria. This was indeed the case, as both NDP52 (Figure 5C) and p62 (Figure 5D) localization to bacteria were significantly reduced by LRSAM1 knockdown at 1 hr postinfection, and expression of LRSAM1 ΔLRR or ΔRING did not rescue adaptor recruitment. LRSAM1 Δ190 (lacking the LRR domain) was also unable to rescue LC3, NDP52, or ubiquitin localization to intracellular *S.* Typhimurium following LRSAM1 depletion (Figure 5E). To further determine if loss of autophagy in the absence of LRSAM1 was dependent on the generation of a ubiquitin signal around bacteria, we examined ubiquitin-independent antibacterial autophagy. We found that the DAG-dependent pathway was unaffected by LRSAM1 knockdown (Figure 5F). Using a previously characterized DAG biosensor (Shahnazari et al., 2010), we cotransfected control, LRSAM1-, or NDP52-targeting siRNA into GFP-LC3 HeLa cells. Following 1 hr of *S.* Typhimurium infection, the proportion of bacteria solely LC3 positive as well as those positive for both LC3 and DAG were scored (Figure 5F). Under LRSAM1- or NDP52-depleted conditions, there was a 7-fold reduction in the ubiquitin-dependent (non-DAG) autophagy pathway. However, the rate of DAG-mediated autophagy (DAG and LC3 double-positive bacteria) was unaffected by either LRSAM1 or NDP52 knockdown (Figure 5F). These data demonstrate that LRSAM1 localizes to intracellular *Salmonella* independently of NDP52 and that LRSAM1 is required for the maintenance of NDP52 around bacteria. Furthermore, LRSAM1 function is required for the ubiquitin-associated autophagy pathway.

## LRSAM1 Is an E3 Ligase that Targets Bacteria

We wished to conclusively establish LRSAM1 as an E3 ligase capable of recognizing and marking bacteria for autophagy via a ubiquitin signal independently of other cellular proteins. Given our results demonstrating that LRSAM1 targeting of bacteria was NDP52 independent, we studied the only known LRSAM1 target, TSG101, a component of the endosomal sorting complex. Knockdown of TSG101 did not result in a significant loss of anti-*Salmonella* autophagy (Figure S3). However, such an approach does not eliminate other possible LRSAM1 partners or accessory proteins. We therefore turned to an in vitro ubiquitination system to definitively establish a role for LRSAM1 as an E3 ligase and define the minimal requirements for its activity. Each reaction contained purified FLAG-LRSAM1 (Figure 6A), recombinant E1 (UBA1) and E2 enzymes, HA-tagged ubiquitin, ubiquitination buffer, and *Salmonella*. We supplied recombinant, purified HA-ubiquitin in *trans*, thus ensuring all ubiquitination occurred in vitro. We identified the necessary E2-conjugating enzymes by screening six putative LRSAM1-interacting E2s identified from published proteomic data sets (Lim et al., 2006; Rual et al., 2005; Stelzl et al., 2005) (Figure 6B). LRSAM1-mediated ubiquitination was predominantly confined to the bacterial pellet and required E1, UBE2D2 or UBE2D3, and LRSAM1 itself (Figures 6B and 6C). Consistent with our in vivo staining, we found that LRSAM1 could also generate robust ubiquitin signals when supplied with *Shigella*, *Listeria*, and AIEC in vitro. LRSAM1 also showed enrichment in the insoluble fraction of bacteria in an LRR-dependent and RING-independent manner (Figures 6D and 6E). Reciprocally, ubiquitination of *Salmonella* required the LRSAM1 RING domain, but not the LRR domain. These data confirmed the roles of the LRR and RING domains established by our observations of LRSAM1

truncations in infected cells (Figures 2 and 3), namely localization and ubiquitination, respectively. Significantly, LRSAM1 itself was ubiquitinated in a RING-dependent manner, even in the absence of bacterial targets, suggestive of E3 ligase autoubiquitination (Figures 6C and 6D). By performing in vitro ubiquitination reactions using ubiquitin mutants, we found that LRSAM1-driven polyubiquitination favored K6- or K27-linkages (Figure 6F).

Due to the autoubiquitination of LRSAM1 observed in the in vitro assay, we sought to determine whether the bulk of in vitro ubiquitination signal was due to LRSAM1 driving ubiqui-tination around bacteria or due to LRSAM1 being autoubiquitinated. To control for the nontarget-mediated autoubiquitination of E3 ligases that is observed in vitro and has been used to identify RING E3 ligases (Jenkins et al., 2005), we used two complementary approaches: (1)We addedan additional RINGE3 ligase, HRD1, which has no known affinity for bacterial targets, using identical conditions, and (2) we examined bacteria from in vitro reactions for ubiquitination by microscopy. We observed that both LRSAM1 and HRD1 displayed apparent autoubiquitination, and much of this signal was resistant to IsoT treatment, which degrades unanchored ubiquitin chains. In the case of LRSAM1, this signal was RING dependent but LRR independent (Figure 6G). These results were not unexpected since the promiscuity and autoactivity of RING ligases is known, and the HRD1 truncation used in these experiments lacks the native transmembrane domain, thus eliminating at least one possible target-specificity determinant. However, visualization of bacteria following in vitro ubiquitination reactions demonstrated additional bacterial targeting. Notably, wild-type LRSAM1 yielded IsoT-resistant distinct ubiquitin signals localized to bacteria, but no ubiquitin was observed on bacteria incubated with LRSAM1 mutants lacking the RING domain or with HRD1 (Figure 6H). Together these data suggest that bacteria can be targeted with ubiquitin in an LRSAM1-dependent manner.

## LRSAM1 Loss in CMT Decreases Antibacterial Autophagy but Has No Effect on Recruitment of Ubiquitin to Protein Aggregates

A recent report has shown that a cohort of patients with Charcot-Marie-Tooth (CMT) disease lacks expression of LRSAM1 (Guernsey et al., 2010). Loss of LRSAM1 expression is induced by a frameshift that truncates the predicted protein sequence (losing the entire RING domain) and results in no detectable levels of LRSAM1 protein (Figure S4A). LRSAM1 null patientderived lymphoblasts (LCLs) were less able to mediate antibacterial ubiquitination of *S.* Typhimurium SL1344 compared to control cells (Figures 7A and 7B), confirming our results based on LRSAM1 knockdown. However, we were unable to observe replication of SL1344 in LCLs (Figure S4B), suggesting that *S.* Typhimurium is toxic to these cells, as has been previously reported (Ko et al., 2009). Using a less virulent strain of *S.* Typhimurium (NTCC12023) (Clark et al., 2011), we found that LRSAM1 null LCLs are less able to control bacterial replication compared to wild-type cells (Figure 7C). Examination of *S.* Typhimurium NTCC12023 in HeLa cells revealed no apparent alterations in the autophagy of these bacteria compared to SL1344, as indicated by LRSAM1 or NDP52 colocalization (Figure S4C). Although we have previously demonstrated that LRSAM1 is dispensable for responses to inducers of classical autophagy (Ng et al., 2011), we wished to further examine the role of LRSAM1 in the autophagic targeting of nonbacterial targets. Since many neurodegenerative disorders appear to be linked to autophagy of protein aggregates, we postulated that CMT patients might exhibit aggregate-driven autophagic defects. To test this hypothesis, we transfected control and LRSAM1 null cells with an aggregate-inducing protein containing 80glutamine residues fused to mCherry (polyQ80-mCherry). By confocal microscopy, we observed that ubiquitination of polyQ80-mCherry aggregates appeared unaffected in LRSAM1 null cells (Figure 7D); analogous results were seen in LRSAM1 knockdown HeLa cells (Figure S4D). We confirmed these results by western blot (Figure 7E).

These results demonstrate that LRSAM1 is not required for ubiquitination of the tested protein aggregates but plays a crucial role against intracellular *Salmonella*. Currently recognized autophagy defects in human diseases show cell-type specificity, often exhibiting overt phenotypes only in neurons and other highly secretory or active cells (Cadwell et al., 2008; Wong and Cuervo, 2010). LRSAM1 may reflect this trend, with loss of LRSAM1 function in autophagy, receptor endocytosis, and cell adhesion (Amit et al., 2004; Li et al., 2003) showing a combined effect in neurons and leading to CMT neuropathy.

## DISCUSSION

Autophagy represents a key barrier to intracellular bacterial growth and is therefore likely to have been one of the evolutionary drivers of specialized intracellular bacterial adaptations such as actin-based motility (*L. monocytogenes*) or the vacuolar lifestyle (*S.* Typhimurium). The major identified pathway through which bacteria are selected for autophagy relies upon accumulation of ubiquitin around target bacteria, binding of ubiquitinrecognizing adaptor proteins, and finally, recruitment of the autophagic machinery. Here we identify LRSAM1 as the E3 ubiquitin ligase responsible for antibacterial ubiquitin association, the crucial first step in this cascade.

We show that LRSAM1 localizes to a variety of bacteria, both Gram negative and positive, but does not localize to intracellular bacteria capable of autophagy evasion. However, these same autophagy-evading strains do trigger ubiquitination by LRSAM1 in vitro. This finding indicates that autophagy evasion relies on manipulation of host cell components prior to LRSAM1 recognition and is not simply due to escape from autophagic capture. In the case of *L. monocytogenes*, it is likely that reduced listeriolysin O expression in strain 15313 maintains vacuolar integrity and thus shields these bacteria from LRSAM1 recognition (Meyer-Morse et al., 2010). Wild-type *S. flexneri* escapes autophagy via IcsB, preventing Atg5 binding to IcsA, but in the absence of IcsB is vulnerable to autophagy (Ogawa et al., 2005). In the absence of IcsB, LRSAM1 localizes to intracellular shigellae, indicating that LRSAM1 plays a role in targeting these bacteria. Autophagic recognition is a prerequisite for septin caging (Mostowy et al., 2010), and LRSAM1 may be one of the mechanisms that results in septin/autophagic capture of *Shigella*.

Using *S.* Typhimurium as a model, we find that LRSAM1 restricts cytoplasmic replication and is indispensable for ubiquitin-mediated autophagy (Figures 1, 3, and 7). However, LRSAM1 is not involved in the DAG-driven autophagy pathway, nor in the ubiquitination of protein aggregates, indicating that LRSAM1 itself is not simply a general selector of autophagic cargo.

Dissection of LRSAM1 domains showed that the LRR domain was necessary and sufficient for localization to bacterial targets, while the RING domain was required for ubiquitination. This finding was supported by results from in vitro ubiquitination of bacteria (Figure 6). These data also correlate with the recent identification of a cohort of CMT patients carrying mutations resulting in a frameshift within the RING domain of LRSAM1 (Weterman et al., 2012). Expression of proteins mimicking such patient mutations had a dominant-negative effect on the ubiquitination and degradation of TSG101, a known LRSAM1 target, suggesting that this might act as a dominant pathogenic mutation in CMT. The importance of the RING domain in LRSAM1 function in both antibacterial autophagy and neuronal development and homeostasis underlines the importance of LRSAM1 as an E3 ligase in human health. It is possible that these functions are linked, with LRSAM1 playing a role in neuronal autophagy and cargo selection (Tang et al., 2011), but our data using model protein aggregates suggest this is not an essential LRSAM1 function in epithelial cells.

Recently, Thurston et al. (2012) found that NDP52 was recruited to damaged intracellular bacterial vacuoles via interaction with galectin-8. We determined that LRSAM1 directly bound NDP52 and mapped the interaction to the LRR domain of LRSAM1 and the coiled-coil region of NDP52. It is therefore possible that LRSAM1 localization to bacteria might occur subsequent to galectin-8/NDP52 association, with LRSAM1 recognition of NDP52 being the crucial step. We directly ruled out a role for NDP52 in LRSAM1 recruitment by knocking down NDP52 and observing no difference in LRSAM1 localization to *S.* Typhimurium. Finally, our in vitro data show that LRSAM1, E1, and E2 complexes are capable of ubiquitinating bacteria in the absence of all other cellular proteins, strongly indicating that LRSAM1 is itself a bacteria-recognition molecule.

LRSAM1 underwent autoubiquitination in vitro (Figure 6C–6E). Pursuing this finding, we found that the ubiquitin linkages promoted by LRSAM1 were predominantly K6 and K27 based. Interestingly, the linkages considered the most generally abundant (K48 and K63) were among the weakest observed. This is consistent with observations using linkage-specific biosensors in infected cells where multiple ubiquitin linkages were observed around *Salmonella* (van Wijk et al., 2012). Ubiquitin-binding adaptor proteins may also bind differentially to subdomains around the target bacterium (Cemma et al., 2011), indicative that different ubiquitin linkages may underlie such patterns. Both K63 and K27 linkages are generated by Parkin-mediated ubiquitination of VDAC1 in mitophagy (Geisler et al., 2010). These results suggest that the more unusual K6 and K27 linkages might favor autophagy, possibly through enhanced binding of autophagy-related adaptor proteins.

In vitro ubiquitination reactions also showed that individual bacteria localized with ubiquitin following incubation with full-length LRSAM1, but not the ΔRING protein or the E3 ligase HRD1. Under these conditions no SCV membrane or cellular proteins are available, so ubiquitination associated with the bacteria likely occurs on the bacterial surface or via ubiquitination of bound LRSAM1. Immunostaining of these reactions on glass substrates appeared less efficient, with fewer bacteria staining positive for ubiquitin than might be suggested by western blotting. We can only speculate on the reasons for this. This may represent assay-specific effects where surfaceimmobilized bacteria are poorer substrates for the reaction. Some of the signal observed by westerns may be weakly associated with the bacterial surface and may be poorly soluble, thus segregating with the bacterial pellet. It is also likely that there are unidentified cellular factors that increase the efficiency of LRSAM1 action against bacteria in infected cells and that are absent in the minimal in vitro system. Our attempts to identify LRSAM1-ubiquitinated bacterial proteins by mass spectroscopy have been unsuccessful, but we have identified 27 lysines within LRSAM1 showing evidence of ubiquitination (data not shown). This large number (27 of 37 lysines, from 40% total peptide coverage) precludes mutagenesis to eliminate autoubiquitination of LRSAM1. We are therefore unable to definitively state the degree to which autoubiquitination and association of ubiquitinated LRSAM1 contributes to the ubiquitin signal observed around bacterial targets. However, given the broad recognition profile of LRSAM1, it is tempting to speculate that bacterial targets of the LRSAM1 LRR are highly conserved. It is most likely that the LRSAM1 LRR recognizes a conserved signal associated with diverse invasive bacteria and through autoubiquitination generates a robust ubiquitin signal to recruit the autophagic machinery. Such a recognition signal is likely to be bacteria intrinsic, since in vitro experiments showed bacteria-associated ubiquitination in the absence of other cellular factors such as membranes, other PRRs, or galectins. Alternatively, it is possible that LRSAM1, once localized, is highly promiscuous and that bacterial target proteins are diverse and modified nonselectively, resulting in low individual abundance of a broad selection of ubiquitinated bacterial components.

Autophagy is a crucial host defense against intracellular pathogens and restricts bacterial replication to specialized niches. LRSAM1 is a unique E3 ubiquitin ligase, bearing both an LRR and RING domain, which directly recognizes intracellular bacteria, initiating the major ubiquitin-dependent antibacterial autophagy cascade. LRSAM1 therefore represents a pattern and cargo recognition protein that targets intracellular bacteria for autophagic destruction, akin to the role of Parkin in mitophagy (Geisler et al., 2010). Thus, we postulate a network of autophagy-associated E3 ligases that perform cargo selection in a cell- and target-specific fashion, allowing cells to respond to diverse stresses via autophagy.

## EXPERIMENTAL PROCEDURES

### LRSAM1 Truncations and Rescue Modifications

LRSAM1 was cloned into pCMV with an N-terminal triple FLAG tag. Truncations and mutations were performed using a modified Phusion Site-Directed Mutagenesis Kit (New England Biolabs, MA). Rescue of LRSAM1 expression was ensured by three synonymous codon mutations in siRNA target sites. All constructs were sequenced and checked for expression. See Supplemental Experimental Procedures for details.

### RNA Interference and Expression Rescue of LRSAM1

HeLa cells were plated in 12-well plates containing 18 mm glass coverslips at $1 \times 10^5$ cells per well. After 24 hr, 20 pmol modified RNA (Stealth RNAi, Invitrogen, CA) and 250 ng of plasmid DNA (where appropriate) were trans-fected using Lipofectamine 2000 (Invitrogen). See Supplemental Experimental Procedures for details.

### Coimmunoprecipitation

Lysates from cells coexpressing FLAG-Strep2-LRSAM1 or FLAG-Strep2 vector and HA-tagged autophagy proteins were incubated with streptavidin beads for 3 hr and stringently washed. Beads were boiled in loading dye and immunoprecipitated proteins were blotted using appropriate antibodies and fluorescent secondary detection (Odyssey, LI-COR Biosciences).

### Infection Assays

*S*. Typhimurium infections of HeLa cells and gentamycin protection assays were performed as previously described (Huett et al., 2009). Infection of lymphoblast cell lines was performed similarly, using an moi of 30–50 in 6-well plates; after 30 min, antibiotic-free RPMI medium was supplemented to a gentamycin concentration of 50 μg/ml, and cells were incubated for 2 hr before fixation. For lymphoblast gentamycin protection assays, cells were plated in 96-well U-bottom plates at $1 \times 10^5$ cells per well in antibiotic-free RPMI medium and infected with *Salmonella* at an moi of 30–50. After 60 min wells were supplemented with gentamycin-containing RPMI (final concentration 50 μg/ml), and cells were incubated further for indicated times. Lymphoblast infections were performed under identical conditions using SL1344 and NTCC12023 *S*. Typhimurium strains. For colocalization of GFP-LC3, ubiquitin, and autophagy adaptors, we used the wild-type SL1344 pDsRed2 strain. For experiments requiring staining in the red channel, we used bacteria without fluorescent tags, instead using Hoescht 33342 (Invitrogen) to stain for bacterial DNA.

### Immunofluorescence Microscopy

Cells on coverslips were washed twice in PBS before being fixed in ice-cold methanol for 3 min and rehydrated in PBS. Antibody staining was then performed without further permeabilization. Exceptions were for ubiquitin colocalization experiments; here ubiquitin was visualized following formalin fixation and 0.5% saponin permeabilization (Birmingham

et al., 2006). Digitonin permeabilization of live cells for selective cytoplasmic staining of SL1344 dsRed2 was performed as previously described (Malik-Kale et al., 2012) followed by formalin fixation. Lymphoblast cell suspensions were mixed and $1 \times 10^5$ cells spun onto slides using a CytoSpin 3 (Thermo Scientific) and air-dried for 10 min. CytoSpin preparations were fixed with 4% formaldehyde, permeabilized, and stained for ubiquitin as described above. For all samples DNA was stained with Hoechst 33342 (Invitrogen). A 100× lens (Zeiss Axioplan, Carl Zeiss MicroImaging, NY) was used for counting under widefield fluorescence illumination. The total number of bacteria per cell and the number of marker-positive bacteria were assessed in randomly chosen fields with at least 25 cells counted for each condition. The number of marker-positive bacteria was calculated as a percentage of total bacteria. Otherwise, images were captured using a Nikon Spinning Disk Confocal with a 100× TIRF lens and Hamamatsu EMCCD camera. We captured z stacks (step size 0.1 μm) and performed deconvolution and 3D reconstructions as previously described (Vyas et al., 2007). Intensity profiles were generated using ImageJ.

### Purification of LRSAM1

LRSAM1 was purified from FreeStyle 293-F cells (Invitrogen, CA). See Supplemental Experimental Procedures for details.

### In Vitro Ubiquitination

Ubiquitination assays were conducted at room temperature or at 37°C for 60 min. The in vitro reaction included LRSAM1 (1 μM) or HRD1 (Lifesensors) and E2 enzymes (100 nM; Lifesensors, PA), *Salmonella* ($5 \times 10^7$ cells per 100 μl reaction), ubiquitination buffer (50 mM Tris [pH 7.5], 5 mM $MgCl_2$, 2 mM DTT, 2 mM ATP), and HA- or His-tagged free ubiquitin (50 μM) (Boston Biochem, MA). At the end of the reaction, intact *Salmonella* cells were centri-fuged at 14,000 × *g* for 5 min and washed once in PBS. Total cells and reaction mix were analyzed by western blotting. Reactions were stopped by adding EDTA (100 μM), and bacteria were washed two times with PBS. Cells were resuspended in IsoT buffer (50 mM Tris [pH 7.5], 5 mM $MgCl_2$, 2 mM DTT, 100 nM IsoT; LifeSensors). Cells were treated with IsoT for 60 min at 37°C, washed three times, and lysed as above. In some experiments *Salmonella* were subsequently lysed with BugBuster (Merck) plus 0.1 mg/ml lysozyme and benzonase with freeze thaw. Soluble and insoluble fractions were extracted by centrifugation at 14,000 × *g* for 30 min and analyzed by western blotting. Microscopy of bacteria from in vitro reactions was performed by immobilization of bacteria onto poly-L-lysine coated coverslips after preincubation with purified E3 ligases for 1 hr and subsequent washing with PBS before overlaying of reaction mixtures minus the E3 ligases. After reactions were completed, coverslips were washed in PBS before paraformaldehyde fixation and staining as previously described.

### Macrophage Infections

All studies involving animals were approved by the Subcommittee on Research Animal Care, which serves as the Institutional Animal Care and Use Committee as required by Public Health Service Policy on Humane Care and Use of Laboratory Animals and the USDA Animal Welfare Regulations. See Supplemental Experimental Procedures for details.

## Supplementary Material

Refer to Web version on PubMed Central for supplementary material.

## Acknowledgments

The authors thank Karen Bedard, Felix Randow, and Conrad Weihl for the supply of reagents; Agnès Gardet, Skip Virgin, Mihai Netea, Joseph Avruch, and Felix Randow for discussions of the manuscript; Jenny Tam for microscopy advice; Lynda Stuart for assistance with deconvolution software; and Natalia Nedelsky for editorial assistance. NDP52 construction mutants were a gift from Felix Randow. R.J.X., A.H., J.B., and R.J.H. are funded by grants from the National Institutes of Health (R01 DK083756, R01 DK060049, U01 DK062432, and P30 DK043351 to R.J.X.), as well as grants from the Helmsley Trust and the Crohn's and Colitis Foundation of America. Additional funding was provided to A.H. by the Faculty of Medicine and Health Sciences, University of Nottingham.

## REFERENCES

Amit I, Yakir L, Katz M, Zwang Y, Marmor MD, Citri A, Shtiegman K, Alroy I, Tuvia S, Reiss Y, et al. Tal, a Tsg101-specific E3 ubiquitin ligase, regulates receptor endocytosis and retrovirus budding. Genes Dev. 2004; 18:1737–1752. [PubMed: 15256501]

Birmingham CL, Smith AC, Bakowski MA, Yoshimori T, Brumell JH. Autophagy controls Salmonella infection in response to damage to the Salmonella-containing vacuole. J. Biol. Chem. 2006; 281:11374–11383. [PubMed: 16495224]

Braun V, Wong A, Landekic M, Hong WJ, Grinstein S, Brumell JH. Sorting nexin 3 (SNX3) is a component of a tubular endosomal network induced by Salmonella and involved in maturation of the Salmonella-containing vacuole. Cell. Microbiol. 2010; 12:1352–1367. [PubMed: 20482551]

Cadwell K, Liu JY, Brown SL, Miyoshi H, Loh J, Lennerz JK, Kishi C, Kc W, Carrero JA, Hunt S, et al. A key role for autophagy and the autophagy gene Atg16l1 in mouse and human intestinal Paneth cells. Nature. 2008; 456:259–263. [PubMed: 18849966]

Cemma M, Kim PK, Brumell JH. The ubiquitin-binding adaptor proteins p62/SQSTM1 and NDP52 are recruited independently to bacteriaassociated microdomains to target Salmonella to the autophagy pathway. Autophagy. 2011; 7:341–345. [PubMed: 21079414]

Clark L, Perrett CA, Malt L, Harward C, Humphrey S, Jepson KA, Martinez-Argudo I, Carney LJ, La Ragione RM, Humphrey TJ, Jepson MA. Differences in Salmonella enterica serovar Typhimurium strain invasiveness are associated with heterogeneity in SPI-1 gene expression. Microbiology. 2011; 157:2072–2083. [PubMed: 21493681]

Deshaies RJ, Joazeiro CA. RING domain E3 ubiquitin ligases. Annu. Rev. Biochem. 2009; 78:399–434. [PubMed: 19489725]

Geisler S, Holmström KM, Skujat D, Fiesel FC, Rothfuss OC, Kahle PJ, Springer W. PINK1/Parkin-mediated mitophagy is dependent on VDAC1 and p62/SQSTM1. Nat. Cell Biol. 2010; 12:119–131. [PubMed: 20098416]

Guernsey DL, Jiang H, Bedard K, Evans SC, Ferguson M, Matsuoka M, Macgillivray C, Nightingale M, Perry S, Rideout AL, et al. Mutation in the gene encoding ubiquitin ligase LRSAM1 in patients with Charcot-Marie-Tooth disease. PLoS Genet. 2010; 6:e1001081. [PubMed: 20865121]

Huett A, Ng A, Cao Z, Kuballa P, Komatsu M, Daly MJ, Podolsky DK, Xavier RJ. A novel hybrid yeast-human network analysis reveals an essential role for FNBP1L in antibacterial autophagy. J. Immunol. 2009; 182:4917–4930. [PubMed: 19342671]

Jenkins Y, Markovtsov V, Lang W, Sharma P, Pearsall D, Warner J, Franci C, Huang B, Huang J, Yam GC, et al. Critical role of the ubiquitin ligase activity of UHRF1, a nuclear RING finger protein, in tumor cell growth. Mol. Biol. Cell. 2005; 16:5621–5629. [PubMed: 16195352]

Ko DC, Shukla KP, Fong C, Wasnick M, Brittnacher MJ, Wurfel MM, Holden TD, O'Keefe GE, Van Yserloo B, Akey JM, Miller SI. A genome-wide in vitro bacterial-infection screen reveals human variation in the host response associated with inflammatory disease. Am. J. Hum. Genet. 2009; 85:214–227. [PubMed: 19664744]

Kuballa P, Huett A, Rioux JD, Daly MJ, Xavier RJ. Impaired autophagy of an intracellular pathogen induced by a Crohn's disease associated ATG16L1 variant. PLoS ONE. 2008; 3:e3391. [PubMed: 18852889]

Lapaquette P, Glasser AL, Huett A, Xavier RJ, Darfeuille-Michaud A. Crohn's disease-associated adherent-invasive E. coli are selectively favoured by impaired autophagy to replicate intracellularly. Cell. Microbiol. 2010; 12:99–113. [PubMed: 19747213]

Li B, Su Y, Ryder J, Yan L, Na S, Ni B. RIFLE: a novel ring zinc finger-leucine-rich repeat containing protein, regulates select cell adhesion molecules in PC12 cells. J. Cell. Biochem. 2003; 90:1224–1241. [PubMed: 14635195]

Lim J, Hao T, Shaw C, Patel AJ, Szabó G, Rual JF, Fisk CJ, Li N, Smolyar A, Hill DE, et al. A protein-protein interaction network for human inherited ataxias and disorders of Purkinje cell degeneration. Cell. 2006; 125:801–814. [PubMed: 16713569]

Malik-Kale P, Winfree S, Steele-Mortimer O. The bimodal lifestyle of intracellular Salmonella in epithelial cells: replication in the cytosol obscures defects in vacuolar replication. PLoS ONE. 2012; 7:e38732. [PubMed: 22719929]

Meyer-Morse N, Robbins JR, Rae CS, Mochegova SN, Swanson MS, Zhao Z, Virgin HW, Portnoy D. Listeriolysin O is necessary and sufficient to induce autophagy during Listeria monocytogenes infection. PLoS ONE. 2010; 5:e8610. [PubMed: 20062534]

Mostowy S, Bonazzi M, Hamon MA, Tham TN, Mallet A, Lelek M, Gouin E, Demangel C, Brosch R, Zimmer C, et al. Entrapment of intracytosolic bacteria by septin cage-like structures. Cell Host Microbe. 2010; 8:433–444. [PubMed: 21075354]

Ng AC, Eisenberg JM, Heath RJ, Huett A, Robinson CM, Nau GJ, Xavier RJ. Human leucine-rich repeat proteins: a genome-wide bioinformatic categorization and functional analysis in innate immunity. Proc. Natl. Acad. Sci. USA. 2011; 108(Suppl 1):4631–4638. [PubMed: 20616063]

Ogawa M, Yoshimori T, Suzuki T, Sagara H, Mizushima N, Sasakawa C. Escape of intracellular Shigella from autophagy. Science. 2005; 307:727–731. [PubMed: 15576571]

Rioux JD, Xavier RJ, Taylor KD, Silverberg MS, Goyette P, Huett A, Green T, Kuballa P, Barmada MM, Datta LW, et al. Genome-wide association study identifies new susceptibility loci for Crohn disease and implicates autophagy in disease pathogenesis. Nat. Genet. 2007; 39:596–604. [PubMed: 17435756]

Rual JF, Venkatesan K, Hao T, Hirozane-Kishikawa T, Dricot A, Li N, Berriz GF, Gibbons FD, Dreze M, Ayivi-Guedehoussou N, et al. Towards a proteome-scale map of the human protein-protein interaction network. Nature. 2005; 437:1173–1178. [PubMed: 16189514]

Shahnazari S, Yen WL, Birmingham CL, Shiu J, Namolovan A, Zheng YT, Nakayama K, Klionsky DJ, Brumell JH. A diacylglyceroldependent signaling pathway contributes to regulation of antibacterial autophagy. Cell Host Microbe. 2010; 8:137–146. [PubMed: 20674539]

Shaid, S.; Brandts, CH.; Serve, H.; Dikic, I. Ubiquitination and selective autophagy. Cell Death Differ. 2012. in press. Published online June 22, 2012. http://dx.doi.org/10.1038/cdd.2012.72

Smith AC, Cirulis JT, Casanova JE, Scidmore MA, Brumell JH. Interaction of the Salmonella-containing vacuole with the endocytic recycling system. J. Biol. Chem. 2005; 280:24634–24641. [PubMed: 15886200]

Stelzl U, Worm U, Lalowski M, Haenig C, Brembeck FH, Goehler H, Stroedicke M, Zenkner M, Schoenherr A, Koeppen S, et al. A human protein-protein interaction network: a resource for annotating the proteome. Cell. 2005; 122:957–968. [PubMed: 16169070]

Tang B, Seredenina T, Coppola G, Kuhn A, Geschwind DH, Luthi-Carter R, Thomas EA. Gene expression profiling of R6/2 transgenic mice with different CAG repeat lengths reveals genes associated with disease onset and progression in Huntington's disease. Neurobiol. Dis. 2011; 42:459–467. [PubMed: 21334439]

Thurston TL, Ryzhakov G, Bloor S, von Muhlinen N, Randow F. The TBK1 adaptor and autophagy receptor NDP52 restricts the proliferation of ubiquitin-coated bacteria. Nat. Immunol. 2009; 10:1215–1221. [PubMed: 19820708]

Thurston TL, Wandel MP, von Muhlinen N, Foeglein A, Randow F. Galectin 8 targets damaged vesicles for autophagy to defend cells against bacterial invasion. Nature. 2012; 482:414–418. [PubMed: 22246324]

van Wijk SJ, Fiskin E, Putyrski M, Pampaloni F, Hou J, Wild P, Kensche T, Grecco HE, Bastiaens P, Dikic I. Fluorescencebased sensors to monitor localization and functions of linear and K63-linked ubiquitin chains in cells. Mol. Cell. 2012; 47:797–809. [PubMed: 22819327]

Vyas JM, Kim YM, Artavanis-Tsakonas K, Love JC, Van der Veen AG, Ploegh HL. Tubulation of class II MHC compartments is microtubule dependent and involves multiple endolysosomal

membrane proteins in primary dendritic cells. J. Immunol. 2007; 178:7199–7210. [PubMed: 17513769]

Weterman MA, Sorrentino V, Kasher PR, Jakobs ME, van Engelen BG, Fluiter K, de Wissel MB, Sizarov A, Nürnberg G, Nürnberg P, et al. A frameshift mutation in LRSAM1 is responsible for a dominant hereditary polyneuropathy. Hum. Mol. Genet. 2012; 21:358–370. [PubMed: 22012984]

Wong E, Cuervo AM. Autophagy gone awry in neurodegenerative diseases. Nat. Neurosci. 2010; 13:805–811. [PubMed: 20581817]

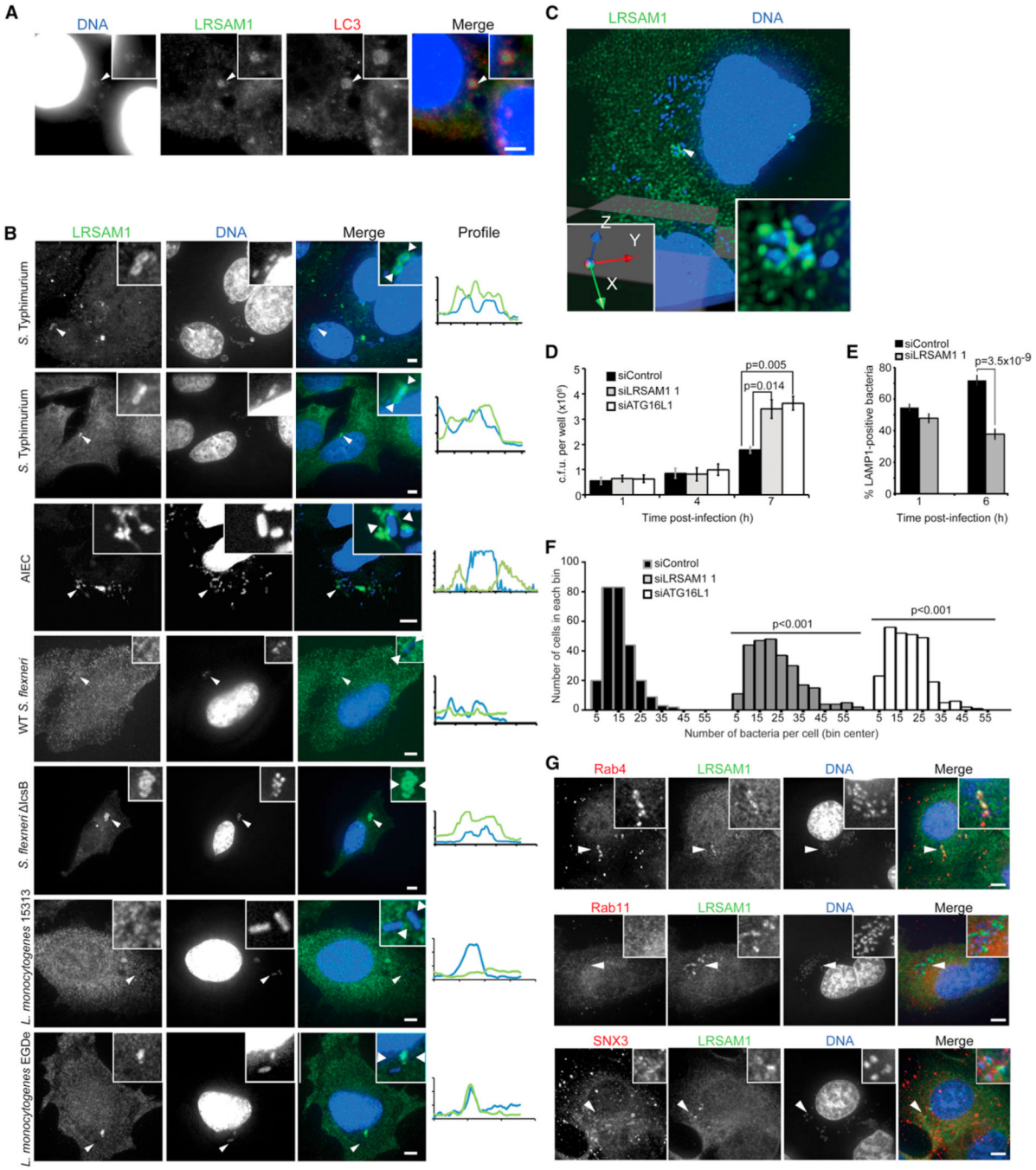


**Figure 1. LRSAM1 Localization to Bacteria and Limitation of Cytoplasmic Growth**

(A–C) Inset features are marked with arrowheads. (A) Colocalization of LRSAM1 (green) and LC3 (red) with bacteria (blue) is observed 45 min following infection of HeLa cells with *S.* Typhimurium SL1344. (B and C) Endogenous LRSAM1 (green) localizes to SL1344, wild-type AIEC, *S. flexneri* ΔIcsB, and *L. monocytogenes* EGDe (DNA, blue) 40 min following infection of HeLa cells. Autophagy-evading wild-type *S. flexneri* and *L. monocytogenes* 15313 did not show LRSAM1 colocalization. Scale bars = 5 μm. (B) Histogram profiles were generated along a line connecting the triangles in merged insets. (C) Rotated, deconvoluted 3D reconstruction of SL1344-infected HeLa cells; x, y, and z indicators are inset.

(D) Viable intracellular *S.* Typhimurium SL1344 in HeLa cells after control siRNA (black), siLRSAM1 1 (gray), or siATG16L1 (white). Data represent means ± SEM, n = 6.
(E) HeLa cells were infected with *S.* Typhimurium SL1344 for 1 or 6 hr and stained for LAMP1. LAMP1-positive bacteria were counted from 24 cells in each of three separate experiments; data were pooled and plotted as a mean percentage of total internalized bacteria ± SEM. No significant differences were observed between control and LRSAM1-depleted samples (n = 72) at 1 hr. At 6 hr, LRSAM1 null samples showed decreased LAMP1-associated bacteria.
(F) HeLa cells transfected with control siRNA, siLRSAM1, or siATG16L1 were stained for bacteria 6 hr following infection with SL1344. Histogram indicates bacterial numbers per cell plotted from data pooled from three independent experiments. The Kolmogorov-Smirnov test with Bonferroni correction was used to assess differences in each of the bacterial distributions compared to siControl-treated cells and showed a significant increase in highly infected LRSAM1- and ATG16L1-depleted cells.
(G) LRSAM1 colocalization with markers of vacuolar maturation in HeLa cells 1hr following infection with SL1344. LRSAM1 (green) localizes to bacteria along with Rab4, but not Rab11 or SNX3 (red). DNA, blue; scale bars = 5 μm. See also Figure S1.

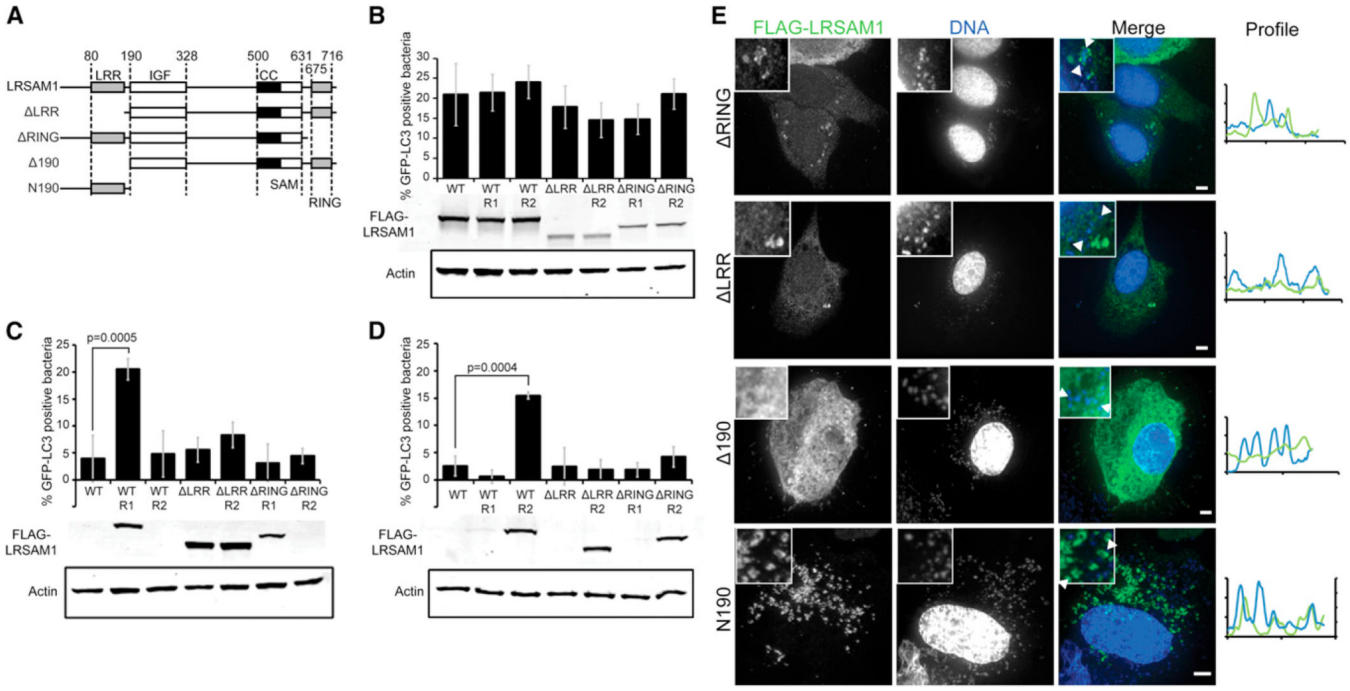


**Figure 2. Roles of LRSAM1 Domains in Autophagy and Localization; Timing of LRSAM1 Recruitment**

(A) Schematic of LRSAM1 and truncated LRSAM1 constructs; LRR (gray), IGF (insulin-like growth factor, white), CC (coiled-coil, black), SAM (sterile alpha motif, white), and RING (gray) domains are shown.

(B–D) Anti-*S.* Typhimurium SL1344 pDsRed2 autophagy in GFP-LC3 HeLa cells cotransfected with control siRNA (B), siLRSAM1 1 (C), or siLRSAM1 2 (D), and FLAG-LRSAM1. Constructs marked R1 or R2 rescue LRSAM1 expression under siRNA1 or siRNA2 conditions, respectively (siRNA1 targets within the LRR domain, so ΔLRR constructs rescue expression under siRNA1 knockdown). FLAG-LRSAM1 expression from full-length and truncated constructs is shown with control anti-actin blots. Data represent means ± SEM, n = 150 infected cells per group. Data in (B) and (C) are pooled from at least two independent experiments.

(E) HeLa cells cotransfected with LRSAM1 siRNA and FLAG-LRSAM1, stained 40 min postinfection. FLAG-LRSAM1 ΔRING (green) localizes to SL1344 (DNA, blue). Neither FLAG-LRSAM1ΔLRR nor LRSAM1 Δ190 localizes toSL1344. The LRR domainof the N190 constructis sufficienttolocalizeto intracellular bacteria. All profiles are shown from a line joining the two arrowheads in merged insets. Scale bars = 5 μm.

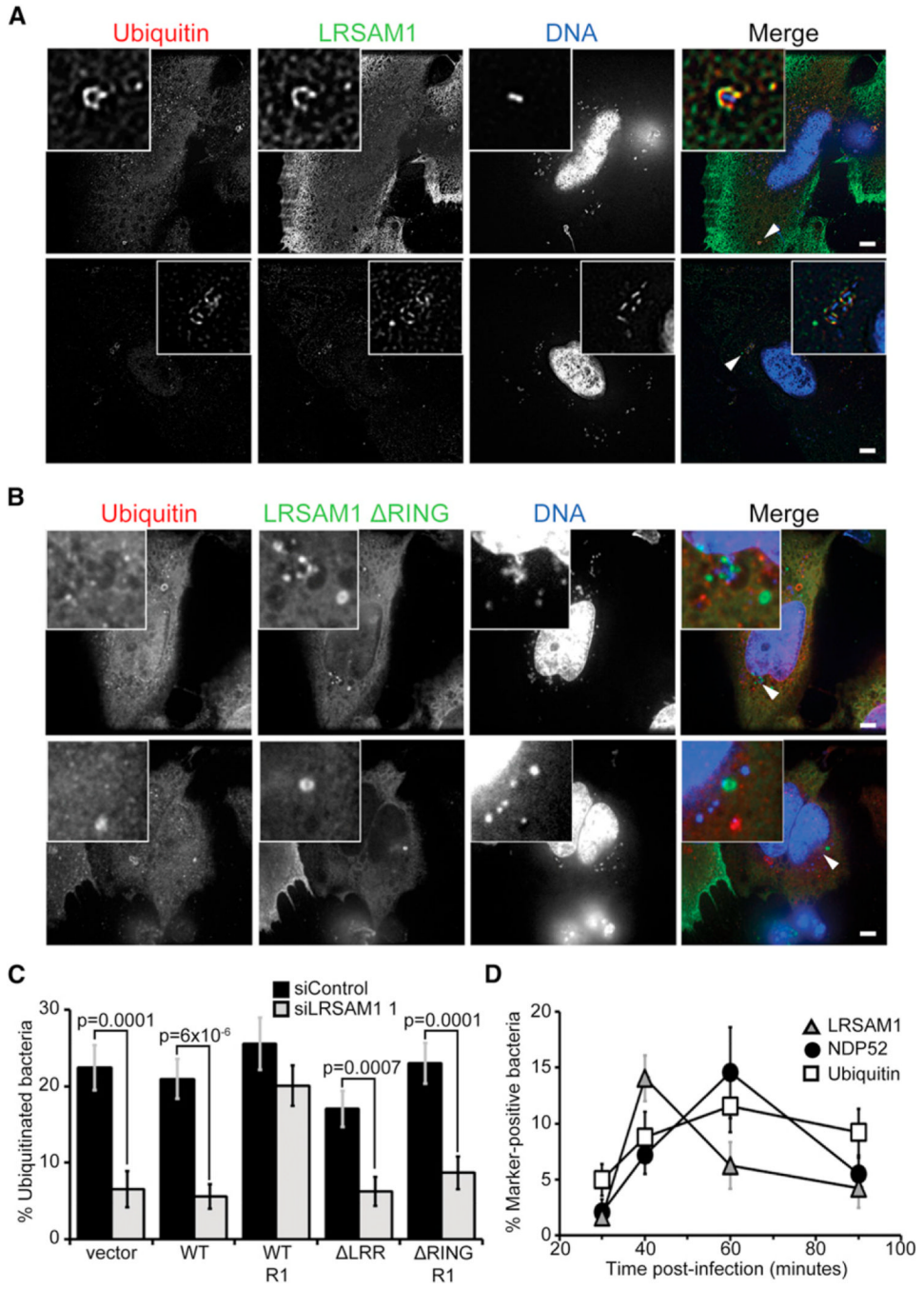


**Figure 3. Bacteria-Associated Ubiquitination**

(A) FLAG-LRSAM1 (green) and endogenous ubiquitin (red) colocalize with SL1344 (DNA, blue) in HeLa cells 40 min following infection; 5 μm scale bar.

(B) FLAG-LRSAM1 ΔRING (green) localizes to *S.* Typhimurium (DNA, blue), but ubiquitin (red) does not colocalize in HeLa cells at 40 min post-infection.

(C) Ubiquitin association with SL1344 pDsRed2 60 min after infection of HeLa cells cotransfected with control siRNA (black) or siLRSAM1 1 (gray) and LRSAM1 rescue constructs. Data represent means ± SEM, n = 75 infected cells per group, data pooled from two independent experiments.

(D) Bacteria/marker colocalization between SL1344 and endogenous LRSAM1 (triangles), GFP-NDP52 (circles), or endogenous ubiquitin (squares) in HeLa cells (n = 60 infected cells per group). Data represent means ± SEM.

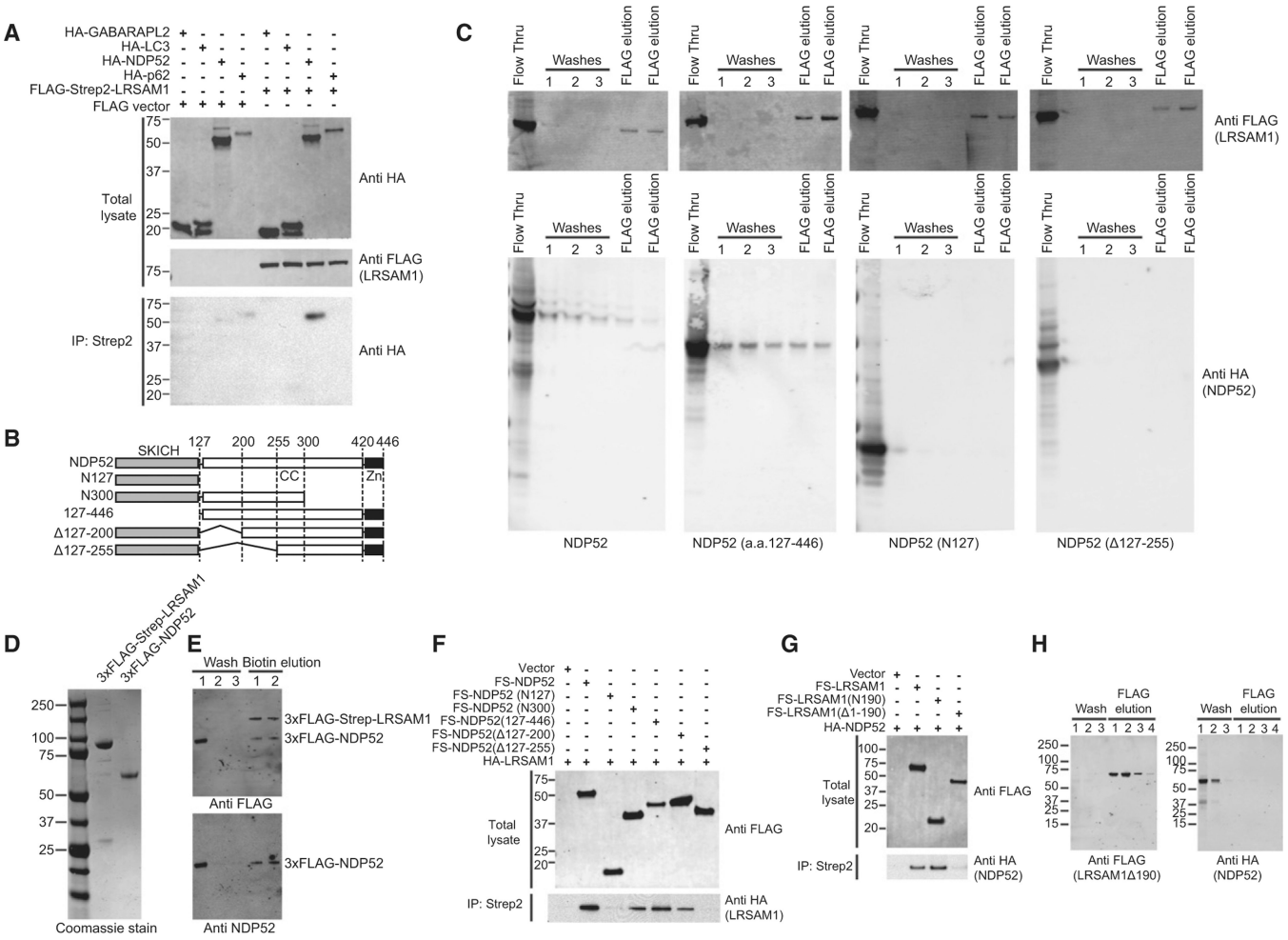


**Figure 4. LRSAM1 Binds NDP52**

(A) HA-NDP52 coprecipitates with FLAG-Strep2-LRSAM1 in cotransfected HEK293T cells; other autophagy proteins tested do not.

(B) NDP52 construct schematics are shown; SKICH (gray), CC (coiled-coil, white), Zn (zinc finger, black).

(C) Purified recombinant FLAG-LRSAM1 was added to 293-F cell lysates expressing HA-NDP52 or mutants. LRSAM1 and bound NDP52 were precipitated with anti-FLAG beads, washed, and LRSAM1 was eluted with FLAG peptide. Washes and elution fractions were blotted for FLAG-LRSAM1 and HA-NDP52.

(D) Coomassie-stained gel showing purified LRSAM1 and NDP52 proteins eluted from anti-FLAG beads prior to mixing and coaffinity purification.

(E) Pure 3×FLAG-Strep-LRSAM1 and 3×FLAG-NDP52 (from [D]) were mixed and then purified over streptavidin beads. Bound protein was eluted with biotin. NDP52 and LRSAM1 coeluted, indicating direct binding.

(F) FLAG-Strep2-NDP52 constructs cotransfected with HA-LRSAM1 in HEK293T cells; NDP52 N127 and Δ127-255 do not bind to LRSAM1.

(G) FLAG-Strep2-LRSAM1 constructs cotransfected with HA-NDP52 in HEK293T cells; LRSAM1 and LRSAM1 N190 bind to NDP52.

(H) Purified recombinant FLAG-LRSAM1 Δ190 was added to 293F cell lysates expressing HA-NDP52. LRSAM1 Δ190 and bound NDP52 were precipitated, eluted, and blotted as in (C). NDP52 was removed by initial washes and did not coelute with LRSAM1 Δ190.

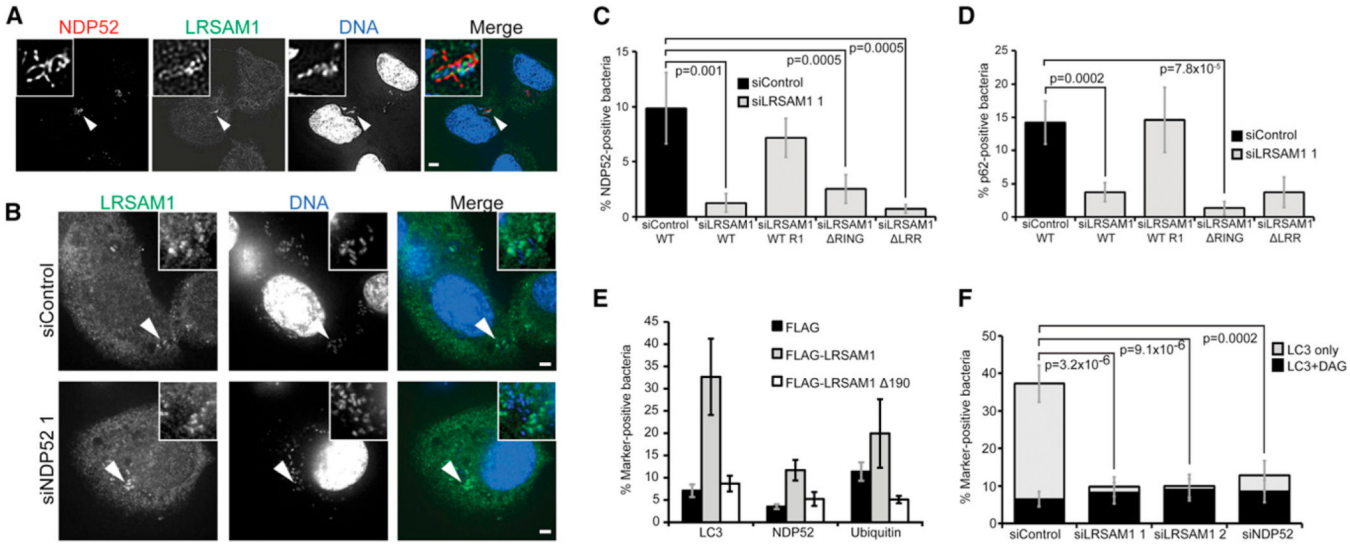


**Figure 5. LRSAM1 Functions Independently of NDP52**

(A) Endogenous LRSAM1 (green) and endogenous NDP52 (red) localize to SL1344 (DNA, blue) in HeLa cells 1 hr postinfection; scale bar = 5 μm.

(B) Control HeLa cells (upper panels)or cells depleted were infected with *S.* Typhimurium (DNA, blue) for1 hrand stained for endogenous LRSAM1 (green). LRSAM1 localization to bacteria was unaffected by NDP52 knockdown. Scale bars = 5 μm.

(C) HeLa cells transfected with either control siRNA and LRSAM1 (black bar) or siLRSAM1 and a full-length LRSAM1 rescue construct (LRSAM1 R1, gray bar) had equal rates of bacteria/NDP52 colocalization. Cells lacking full-length LRSAM1 did not show the same level bacteria/NDP52 colocalization. Data represent means ± SEM, n = 50 infected cells per group.

(D) HeLa cells were cotransfected with GFP-p62 and siRNA along with LRSAM1. Cells were infected 48 hr following transfection. Cells transfected with either control siRNA and LRSAM1 (black bar) or siLRSAM1 and a full-length LRSAM1 rescue construct (LRSAM1 R1, gray bar) had equal rates of bacteria/p62 colocalization. Cells in which LRSAM1 was knocked down, or those expressing truncations lacking either the LRR or RING domains, failed to show the same level of bacteria/p62 colocalization. Data represent means ± SEM, n = 50 infected cells per group.

(E) LRSAM1 knockdown in HeLa cells followed by rescue with empty FLAG vector (black), LRSAM1 (gray) or LRSAM1 Δ190 (white). Only full-length LRSAM1 restored LC3, NDP52 and ubiquitin localization to *Salmonella*. Data represent means ± SD, n = 50, data pooled from 2 independent experiments.

(F) HeLa cells stably expressing GFP-LC3 were transfected with siRNA against LRSAM1 or NDP52. The percentage of GFP-LC3$^+$ bacteria (ubiquitin-dependent pathway, gray) or GFP-LC3$^+$ DAG$^+$ bacteria (ubiquitin independent pathway, black) are shown. Data represent means ± SEM, n = 50 infected cells per group, pooled from 2 independent experiments. See also Figure S2 and Movie S1.

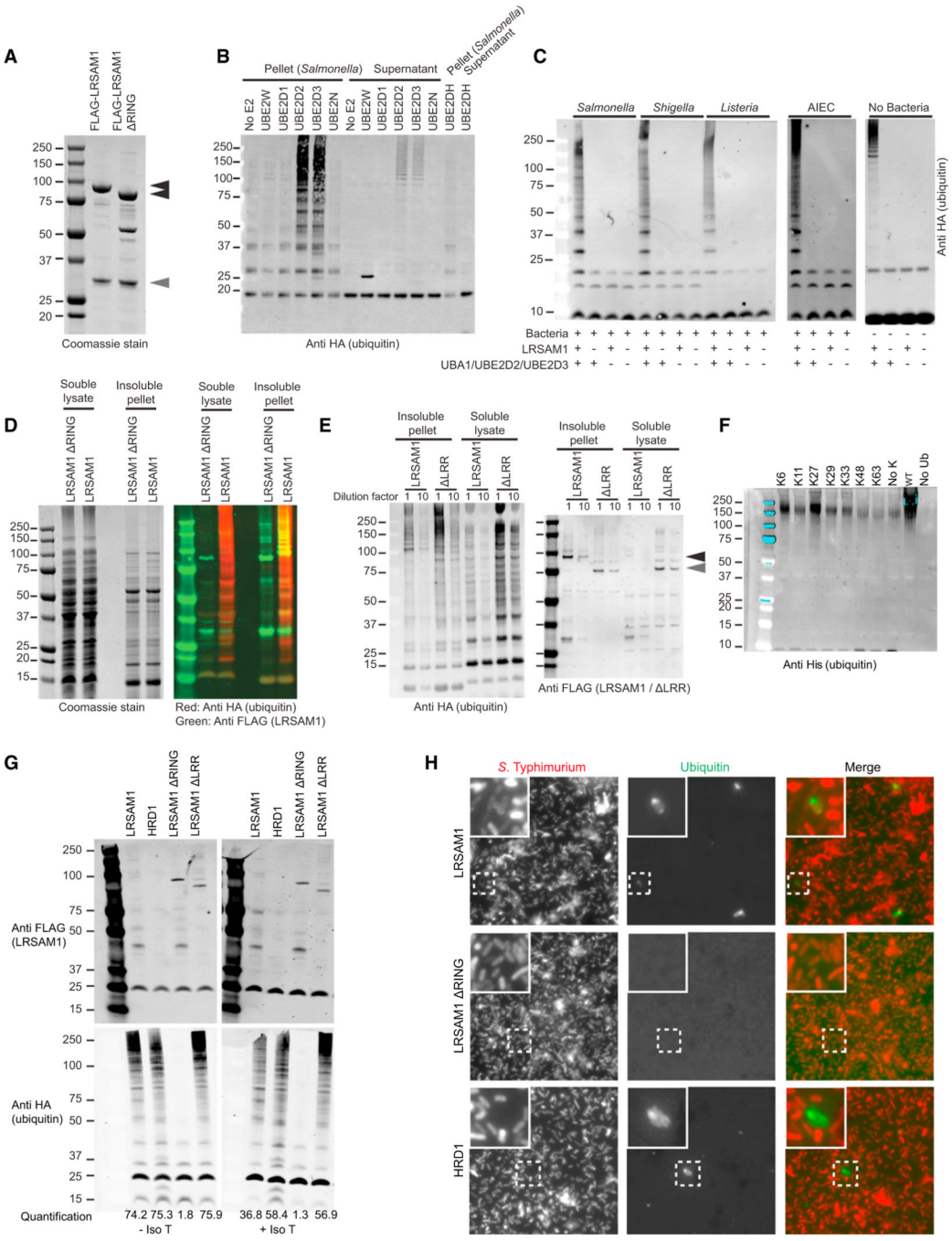


**Figure 6. LRSAM1-Dependent In Vitro Ubiquitination of Bacteria**

(A) Coomassie staining of recombinant FLAG-LRSAM1 proteins following purification. Full-length proteins (black arrows) and a cleavage/degradation product (gray arrow) are shown.

(B) Western blot of in vitro ubiquitination reactions. LRSAM1-driven ubiquitination of *Salmonella* requires UBE2D2 or UBE2D3, and ubiquitinated proteins are largely confined to the bacterial fraction.

(C) LRSAM1-dependent in vitro ubiquitination is capable of targeting *S.* Typhimurium, *S. flexneri*, *L. monocytogenes* 15313, and AIEC.

(D) Following in vitro ubiquitination of *Salmonella*, the majority of protein is located in the soluble lysate fraction (Coomassie stain, left panel). However, the majority of LRSAM1 (green signal, right panel) is located in the insoluble fraction. This LRSAM1 protein shows ubiquitin laddering and colocalizes with HA-ubiquitin (red signal, overlap shown as yellow) in a RING-dependent manner, indicating RING-dependent autoubiquitination.
(E) Western blots of pellets and lysates from in vitro *Salmonella* ubiquitination reactions. In the absence of the LRR domain, LRSAM1 is capable of ubiquitination (left panel). However, LRSAM1 ΔLRR fails to completely localize to the insoluble fraction of the bacterial pellet (right panel, black arrow), remaining in the supernatant (gray arrow).
(F) In vitro *Salmonella* ubiquitination reactions each performed with a unique His-tagged ubiquitin mutant. Lysine-less ubiquitin (No K) represents mono-ubiquitination.
(G) Western blots of in vitro *Salmonella* ubiquitination reactions. Whole lysates of bacteria incubated with LRSAM1, LRSAM1 mutants, or HRD1. Quantification of total ubiquitin signals shows RING-dependent LRSAM1 activity, but extensive nonspecific activity occurs, leading to high levels of HRD1-mediated ubiquitination.
(H) *S.* Typhimurium SL1344 preincubated with LRSAM1 or HRD1 were immobilized on poly-L-lysine-coated coverslips, followed by addition of additional reaction components with incubation for 1 hr at 37°C. Subsequent IsoT treatment was used for 1 hr at room temperature. Following washing, bacteria were stained by ubiquitin. See also Figure S3.

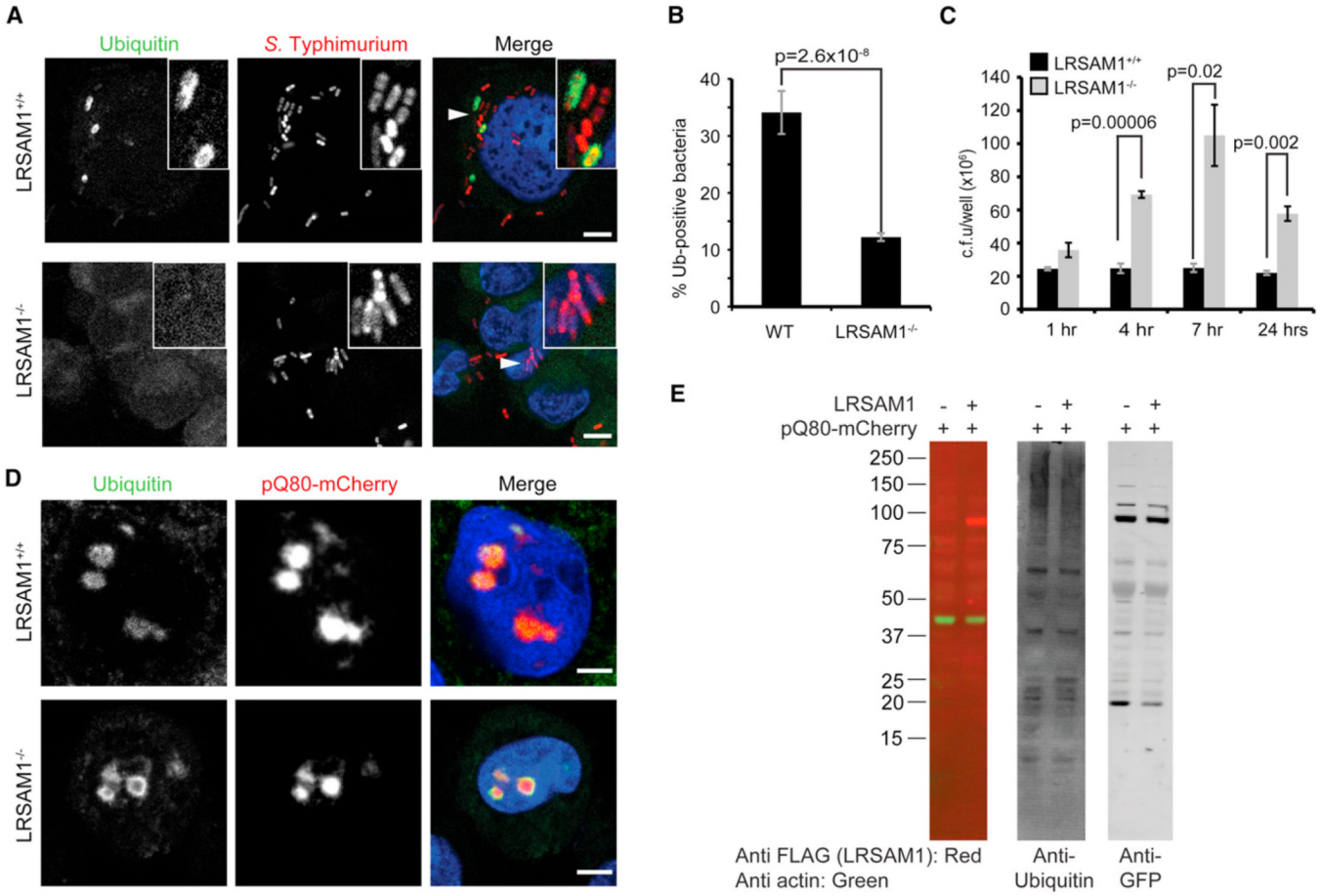


**Figure 7. LRSAM1-Deficient Cells from CMT Patients Phenocopy LRSAM1 Knockdown**

(A) Ubiquitination ofSL1344 pDsRed2inhuman lymphoblasts from LRSAM1-deficientorcontrol donors. Endogenous ubiquitin (green) and SL1344 pDsred2 (red) are shown with DNA (blue) following 1 hour of infection; scale bar = 5 μm.

(B) Quantification of bacterial ubiquitination at 60 min postinfection in LRSAM1-deficient and -replete lymphoblasts. Data represent means ± SEM, n = 150 infected cells per group.

(C) Viable intracellular *Salmonella* (strain NTCC12023) replicate in lymphoblasts derived from LRSAM1-deficient patients (gray), but not in cells from healthy controls (black). Data represent means ± SEM, n = 6.

(D) Ubiquitination (green) of polyQ80-mCherry aggregates (red) is normal in LRSAM1-deficient human lymphoblasts. DNA, blue; scale bars = 5 μm.

(E) Western blot against ubiquitin and mCherry showing similar levels of ubiquitination in LRSAM-deficient and control lymphoblasts. See also Figure S4.